

Atomic Interferometer with Amplitude Gratings of Light and Its Applications to Atom Based Tests of the Equivalence Principle

Sebastian Fray,¹ Cristina Alvarez Diez,^{1,2} Theodor W. Hänsch,^{1,2} and Martin Weitz³

¹Max-Planck-Institut für Quantenoptik, 85748 Garching, Germany

²Sektion Physik der Universität München, 80799 München, Germany

³Physikalisches Institut der Universität Tübingen, 72076 Tübingen, Germany

(Received 18 February 2004; published 8 December 2004)

We have developed a matter wave interferometer based on the diffraction of atoms from effective absorption gratings of light. In a setup with cold rubidium atoms in an atomic fountain the interferometer has been used to carry out tests of the equivalence principle on an atomic basis. The gravitational acceleration of the two isotopes ⁸⁵Rb and ⁸⁷Rb was compared, yielding a difference $\Delta\mathbf{g}/\mathbf{g} = (1.2 \pm 1.7) \times 10^{-7}$. We also perform a differential free fall measurement of atoms in two different hyperfine states, and obtained a result of $\Delta\mathbf{g}/\mathbf{g} = (0.4 \pm 1.2) \times 10^{-7}$.

DOI: 10.1103/PhysRevLett.93.240404

PACS numbers: 03.75.Dg, 04.80.Cc, 39.20.+q, 42.50.Vk

Optical fields can be used to coherently split and recombine atomic de Broglie waves [1–3]. To date, atomic interferometry has allowed for impressive precision measurements of Earth's gravitation [4]. Einstein's weak equivalence principle states that all bodies, regardless of their internal composition, are affected by gravity in an universal way, i.e., in the absence of other forces they fall with the same acceleration. For macroscopic (i.e., classical) objects, tests of the equivalence principle have been performed since the early days of modern physics [5]. Investigations of the equivalence principle on an atomic basis have been proposed [6], motivated by the quest to provide new tests of theories which merge quantum mechanics and relativity.

Here we report of an experiment demonstrating a test of the equivalence principle with quantum probe particles based on atom interferometry. Our experiment uses the two stable isotopes of the rubidium atom with nearby optical transition wavelength. For our measurements, we have developed a light pulse atom interferometer based on the diffraction of atoms from standing optical waves acting as effective absorption gratings. By comparing the free fall of the two distinct isotopes ⁸⁵Rb and ⁸⁷Rb, we have measured their differential acceleration in Earth's gravitational field to a relative accuracy of 1.7×10^{-7} . Further, we have tested for a variation of the measured free fall acceleration as a function of relative orientation of nuclear to electron spin to a differential accuracy of 1.2×10^{-7} by comparing interference patterns measured with ⁸⁵Rb atoms prepared in two different hyperfine ground states. Within the quoted uncertainties, the results in both of our measurements are consistent with an isotope and internal state independent gravitational acceleration. We expect that technical improvements will in the future allow for very critical tests of the equivalence principle on an atomic basis.

Before proceeding, we note that the first atom based tests of general relativity are the famous Pound-Rebka

experiments, which are sensitive to the gravitational redshift. For a comparison of different tests of the equivalence principle, see [7]. To date, this tiny shift (of order $\Delta hg/c^2$) has been verified to an accuracy of 10^{-4} [8]. We also wish to point out that theoretical work has discussed the possibility of a spin-gravitational coupling [9]. Such theories have so far only been tested with macroscopic matter [10].

When comparing the free fall of different atomic species or atoms in different internal states, it seems advantageous to use techniques which are only weakly dependent on a specific internal atomic structure. In the to date most absolute atomic interferometric measurement of gravitation [4], beam splitters based on off-resonant Raman transitions were used which change both the internal and external degrees of freedom. Another class of atom interferometers only involve interference of the external degrees of freedom, as have, e.g., been realized with off-resonant standing waves acting as phase gratings [11].

Our scheme for atomic interferometry is shown in Fig. 1. The atomic beam splitters are realized with pulsed standing waves tuned resonantly to an open transition from a ground state $|g_D\rangle$ to a spontaneously decaying excited state $|e\rangle$. After the pulses only atoms in state

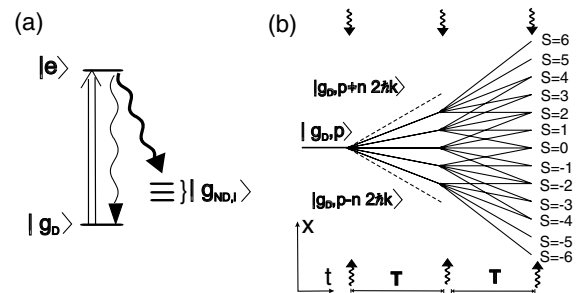


FIG. 1. (a) Simplified level scheme and (b) recoil diagram of an atomic interferometer realized with three effective absorption gratings of light.

$|g_D\rangle$ are detected. For an incident atom distribution, the standing wave fields will lead to a spatially dependent pumping, and atoms passing near the antinodes will preferentially be "removed" into states $|g_{ND,i}\rangle$, which are not detected, while atoms near the nodes will remain in state $|g_D\rangle$. The transient standing wave thus acts as an effective absorption grating of spatial periodicity $\lambda/2$, on which an incident plane atom wave $|g_D, \vec{p}\rangle$ with internal state $|g_D\rangle$ and momentum \vec{p} is diffracted into a series of components $\dots, |g_D, \vec{p} - 2\hbar\vec{k}\rangle, |g_D, \vec{p}\rangle, |g_D, \vec{p} + 2\hbar\vec{k}\rangle, \dots$. For an increased pulse energy, the open fraction of the effective grating lessens, which results in a larger number of generated paths.

Since only resonant light is used, we do not expect phase shifts between adjacent paths due to the ac Stark effect. While diffraction from a single effective optical absorption grating has been demonstrated [12], the extension to an atomic interferometer is not obvious since the spontaneous emission occurring during the beam splitting process may *a priori* affect the coherence, which would destroy the observed interference contrast. The operation of our atom interferometer demonstrates that this is not the case, which intuitively can be seen by noting that the use of an open optical transition ensures that, assuming a favorable branching ratio, which-path information is only present for atoms that have undergone an optical pumping event. Our experiment relies on a rubidium atomic fountain, in which a temporal sequence of three resonant optical standing wave pulses is applied to coherently split and redirect the wave packets, and finally readout the atomic interference pattern. The diameter of the pulsed optical beams is sufficiently large that each pulse affects the whole atomic cloud.

In our experiment, the ground state $|g_D\rangle$ was chosen to be a magnetic field insensitive ($m_F = 0$) Zeeman sublevel of a rubidium ground state hyperfine component (i.e., $F = 2$ or $F = 3$ for ^{85}Rb , or $F = 1$ for ^{87}Rb). The standing wave is σ^+ polarized and tuned resonantly to a hyperfine component of the rubidium D1-line. An atom interferometer is realized with a sequence of three such optical pulses. The first standing wave pulse at $t = 0$ splits an atomic wave packet into several distinct paths. At a time $t = T$ second pulse is applied, which again leads to a diffraction and coherently splits up the paths. At time $t = 2T$, several paths spatially overlap in a series of families of wave packets. We expect that the wave nature leads to a spatial atomic interference structure. To read out this periodic fringe pattern, we again apply a resonant optical pulse tuned to the open transition. The periodic pattern could now be read out by scanning the position of this third grating and monitoring the number of transmitted atoms in state $|g_D\rangle$. For technical reasons, we actually leave the position of the optical grating constant and instead vary the pulse spacing T , which due to Earth's gravitational acceleration also allows us to observe the fringe pattern.

We shall now outline the calculation of the interference pattern (see also [2]). The Hamiltonian of the system is assumed to be $H = \vec{p}^2/2m + (\hbar\omega_{eg} - i\hbar\Gamma/2)|e\rangle\langle e| - e\vec{r} \cdot \vec{E}$ where $\hbar\omega_{eg}$ denotes the atomic energy spacing between level $|g_D\rangle$ and $|e\rangle$. The relaxation of the excited state is accounted for by introducing a non-Hermitian decay term $-(i\hbar\Gamma/2)$. This neglects the decay into the levels $|g_D\rangle$. In the case of negligible branching ratio of the decay into $|g_D\rangle$ the above Hamiltonian would allow for an exact description of the observed fringe pattern. Otherwise, we expect an additional incoherent background to the fringes. The standing wave electric field is assumed to be $\vec{E} = \vec{E}_0 \cos(\vec{k}\vec{r} - \omega t) + \vec{E}_0 \cos(-\vec{k}\vec{r} - \omega t)$.

We shall first consider the atomic response to a single pulse of the standing wave field. Assume that the pulse length τ is so short that we can neglect the phase evolution due to the kinetic energy term (Raman-Nath regime [1]). A plane atomic wave with initial internal and external states $|g_D, \vec{p}\rangle$ is then diffracted into the coherent superposition of paths

$$|\Psi\rangle = \sum_{n=-\infty}^{\infty} \exp\left(-\frac{\Omega^2}{\Gamma} \tau_1\right) I_n\left(-\frac{\Omega^2}{\Gamma} \tau_1\right) |g, \vec{p} + 2n\hbar\vec{k}\rangle,$$

where $\Omega = e\vec{E}_0\langle g|\vec{r}|e\rangle\hbar$ denotes the Rabi frequency and $I_n(x)$ the modified Bessel function. Unlike the "usual" Bessel functions $J_n(x)$, which describe diffraction by an off-resonant standing wave, the functions $I_n(x)$ do not oscillate with x . Because of this property optical absorption gratings are promising tools for future multiple-beam atom interferometers with a large number of paths [13,14]. The approximate atom loss equals the "open ratio" of the effective absorption grating, and is of the order of $1/N$ for an N -path beam splitter.

Using the above Hamiltonian one can calculate the momentum picture wave function directly before the third (readout) pulse. We are interested in the atomic response for a broad velocity distribution, for which the velocity width along \vec{k} is large compared to $1/(k \cdot T)$. In the expression for the spatial density $\rho_D(x) = \int g(p) \cdot \langle x|\psi\rangle \times \langle \psi|x\rangle dp$ of atoms in state $|g_D\rangle$, we can solve the integral and simplify the resulting expression to $\rho(x) = \sum_{s=-\infty}^{\infty} \|\Psi_s(x)\|^2$, where

$$|\Psi_s\rangle = \sum_{n=-\infty}^{\infty} I_n\left(-\frac{\Omega^2}{\Gamma} \tau_1\right) I_{s-2n}\left(-\frac{\Omega^2}{\Gamma} \tau_2\right) \times e^{-(\Omega^2/\Gamma)(\tau_1+\tau_2)} \times e^{i(sn-n^2)2\omega_r T} e^{-in2\vec{k}\vec{x}}.$$

Here, $s = 2n + l$ and $\omega_r = 2\hbar k^2/m$ denotes the recoil energy of a two-photon transition in frequency units. In the presence of a gravitational field, we obtain an additional phase term $-in \vec{k} \vec{g} T^2$ in the exponential factor. While the expected density modulation is near sinusoidal in the unsaturated case [i.e., $(\Omega^2/\Gamma)\tau_i \lesssim 1$], the fringe pattern sharpens to an Airy-function-like multiple-beam pattern for larger pulse energies [15].

Our experimental setup is based on a ultrahigh vacuum chamber, in which 2×10^9 atoms (^{85}Rb or ^{87}Rb , respectively) are initially captured in a magneto-optical trap and accelerated by an upwards traveling optical molasses. The temperature of the atoms at this point is $6 \mu\text{K}$. After the launch, a homogeneous 50 mG magnetic bias field oriented parallel to the optical interferometer beams is activated. While the atoms travel on a fountain-type ballistic trajectory, a series of beam splitting pulses is applied from the optical interferometer beams. Before and after the interferometric pulses we select the $m_F = 0$ component of the corresponding hyperfine state by an appropriate sequence of microwave π pulses and a resonant optical pulse removing residual population. The atomic signal is then measured with a FM-fluorescence detection method, for which the atoms were irradiated with a resonant modulated optical beam. The cold atoms convert the frequency modulation into an amplitude modulated fluorescence, which is phase-sensitively detected. This method was developed to selectively detect the signal of cold atoms in the presence of a thermal rubidium background vapor. Further improvements on the signal to noise ratio would be possible with a differentially pumped vacuum chamber.

The optical interferometer pulse sequence is generated by an injection locked master-slave diode laser system operating near 795 nm and a passage through two acousto-optic modulators. The light is coupled into a single mode optical fiber, expanded to a 3 cm Gaussian beam diameter and coupled into the vacuum chamber. After the transmitting the chamber, the beam is retro-reflected with a mirror. The generated (pulsed) optical standing wave irradiating the cold atoms is oriented vertically, and has an intensity of $3 \text{ mW}/\text{cm}^2$ per direction. The retroreflection mirror is passively vibration isolated by suspending the mirror on a 2.5 m long ribbon string.

The atom interferometer as shown in Fig. 1 is realized applying a temporal sequence of three resonant standing wave pulses to the cold atoms. The length of an optical beam splitting pulse is 200 ns. We observe fringe patterns with good signal to noise up to interrogation times near $T = 40$ ms. Figure 2 shows typical atomic signals as a function of pulse spacing T between the optical beam splitting pulses. The observed fringe contrast is 20% for small interrogation times T and reduces to some 9% for the shown fringe patterns with high gravitational sensitivity recorded near $T = 40$ ms. This loss of fringe contrast for longer coherence times is attributed to residual mechanical vibrations of the interferometer beams retro-reflecting mirror. The widths of the observed principal maxima is between $0.4 \cdot 2\pi$ and $0.5 \cdot 2\pi$. The former value was reached when using longer optical pulse lengths, which however lessened the signal amplitude. We attribute this mainly to residual reflection of the optical vacuum windows, which cause an intensity imbalance between forward and backward running wave of some 2%. The imperfect window transmission of our

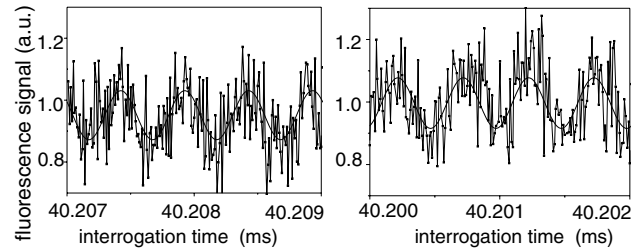


FIG. 2. Typical interference signals as a function of pulse spacing T varied in narrow regions near $T = 40$ ms. The signals were recorded for (a) ^{85}Rb atoms with the optical field tuned to the $F = 2 \rightarrow F' = 3$ component near the 1195th revival and for (b) ^{87}Rb atoms using $F = 1 \rightarrow F' = 2$ component of the rubidium D1-line near the 1167th revival, respectively. In the presence of Earth's gravitational field an observation of the interference pattern is possible by a variation of the interrogation times. Each data point corresponds to the signal recorded in a single fountain launch. The solid lines are fits to sinusoidal functions.

present apparatus is attributed to contamination with adsorbed rubidium from the background vapor. Applying a white light desorption method [16] lowers the disturbing reflection from six to the above quoted value of 2%. We were, however, not able to completely remove the contamination. It is anticipated that the residual intensity imbalance also reduces the fringe contrast from an theoretical value near 100% for the used transition to the experimentally observed value at small drift times T .

To determine the total phase shift between the interfering paths induced by Earth's gravitational field, we have analyzed fringe patterns recorded for different pulse spacings T , which avoids any phase ambiguity caused by the periodic character of the pattern. Figure 3 shows typical recorded data (dots) along with a fit to the expected parabolic curve (solid), while the gravitational acceleration g was left as a free parameter. From the fringe patterns recorded at $T = 40$ ms interrogation time, we at present can determine Earth's gravitational acceleration to a statistical accuracy of 8×10^{-8} in six hours of data acquisition. It is anticipated that the implementation of an active vibration isolation stage, as used in Ref. [4], would allow for longer interrogation times and yield a comparable statistical accuracy for measurements of the gravitational phase.

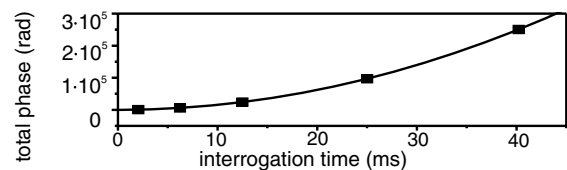


FIG. 3. Total atom phase between adjacent paths of the ^{85}Rb interferometer as a function of interrogation time T . The solid line represents a parabolic fit. The used atomic levels were as in Fig. 2(a).

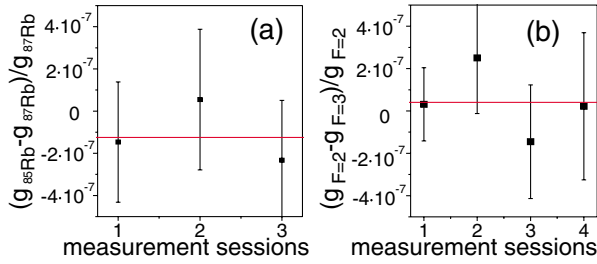


FIG. 4 (color online). Measured difference of the gravitational acceleration in individual measurement sessions (dots) and total average (vertical line) for (a) the two different isotopes ^{85}Rb and ^{87}Rb and (b) for atoms (^{85}Rb) in the different hyperfine ground states $F = 2$ and $F = 3$.

We have compared the gravitational acceleration experienced by ^{85}Rb atoms in the $F = 2, m_F = 0$ hyperfine ground state with that of ^{87}Rb atoms in $F = 1, m_F = 0$. For this atom based test of the equivalence principle, we recorded series of fringe patterns with $T \approx 40$ ms for the two different isotopes. The data were recorded in three measurement sessions, each corresponding to the data recorded during 1 d. Fringe patterns have for both measurements already been shown in Fig. 2. Figure 4(a) shows the measured averaged values of $(\mathbf{g}_{^{85}\text{Rb}} - \mathbf{g}_{^{87}\text{Rb}})/\mathbf{g}_{^{85}\text{Rb}}$ in the three measurement sessions along with a vertical line representing the total average. This final value for the difference is $(\mathbf{g}_{^{85}\text{Rb}} - \mathbf{g}_{^{87}\text{Rb}})/\mathbf{g}_{^{85}\text{Rb}} = (1.2 \pm 1.7) \times 10^{-7}$. The quoted statistical error here equals the (estimated) total uncertainty. In our differential measurement, systematic errors due to misalignment of the beams, wave front curvature, and Coriolis forces largely cancel, and at the present level of accuracy clearly can be neglected. Moreover, as all paths of our atom interferometer are in the same internal state, systematic effects due to the second order Zeeman shift occur only in the presence of a magnetic field gradient. The estimated systematic uncertainty due to field inhomogeneities (8 mG/cm) is for our present apparatus estimated to be 5×10^{-11} , which is also clearly negligible. Within the quoted uncertainties, our above given value agrees well with the expected result of an identical gravitational acceleration of the two rubidium isotopes.

We have furthermore compared the gravitational acceleration experienced by atoms (^{85}Rb) in the two different hyperfine ground states $F = 2, m_F = 0$ and $F = 3, m_F = 0$. For the latter measurement, the optical interferometer beams were tuned to the $F = 3 \rightarrow F' = 3$ hyperfine component of the D1 line. Our experimental results for the measured relative differential gravitational acceleration is summarized in Fig. 4(b). Our averaged, final result here is $(\mathbf{g}_{F=3} - \mathbf{g}_{F=2})/\mathbf{g}_{F=2} = (0.4 \pm 1.2) \times 10^{-7}$. Within the quoted uncertainty, we do not observe a difference in Earth's gravitational acceleration for atoms in the two hyperfine states. Our atom interferometer in a

very natural way allows for a comparison of results that are based on different atomic states. An important question for future theoretical work is to investigate to what extent such a measurement of gravitational acceleration of atoms in two different internal states is complimentary to atomic clock experiments of the Pound-Rebka type.

To conclude, we have demonstrated an atom interferometer based on pulsed, effective absorption gratings of light. We have applied the interferometer to demonstrate novel atom based test of the equivalence principle.

For the future, improvements in wave front quality and a better vibrational isolation can yield longer coherence times, and furthermore allow for multiple-beam interference signals with sharp principal maxima where in contrast to earlier schemes the path number is not limited by the internal atomic structure [13,14]. Furthermore, we anticipate that atom interferometry will allow for very critical test of the equivalence principle on an atomic basis.

We acknowledge discussions with C. Lämmerzahl, C. J. Bordé, and R. Chiao. This work was supported in parts by the Deutsche Forschungsgemeinschaft.

-
- [1] See, e.g., P. Berman, *Atom Interferometry* (Academic Press, San Diego, 1997).
 - [2] V. P. Chebotayev *et al.*, *J. Opt. Soc. Am. B* **2**, 1791 (1985).
 - [3] C. J. Bordé, *Phys. Lett. A* **140**, 10 (1989).
 - [4] A. Peters, C. Keng Yeow, and S. Chu, *Nature (London)* **400**, 849 (1999).
 - [5] Y. Su *et al.*, *Phys. Rev. D* **50**, 3614 (1994).
 - [6] J. Audretsch, U. Bleyer, and C. Lämmerzahl, *Phys. Rev. A* **47**, 4632 (1993); L. Viola and R. Onofrio, *Phys. Rev. D* **55**, 455 (1997).
 - [7] K. Nordtvedt, gr-qc/0212044.
 - [8] R. F. C. Vessot *et al.*, *Phys. Rev. Lett.*, **45**, 2081 (1980).
 - [9] C. Lämmerzahl, in *Proceedings of the International School of Cosmology and Gravitation, Course XV*, edited by P. G. Bergmann *et al.* (World Scientific, Singapore, 1998), and references therein.
 - [10] C. H. Hsieh *et al.*, *Mod. Phys. Lett. A* **4**, 1597 (1989).
 - [11] E. M. Rasel *et al.*, *Phys. Rev. Lett.* **75**, 2633 (1995); D. M. Giltner, R. W. McGowan, and S. A. Lee, *ibid.* **75**, 2638 (1995); S. B. Cahn *et al.*, *ibid.* **79**, 784 (1997); S. Gupta *et al.*, *ibid.* **89**, 140401 (2002).
 - [12] A. P. Chu, K. S. Johnson, and M. G. Prentiss, *Opt. Commun.* **134**, 105 (1997); M. K. Oberthaler *et al.*, *Phys. Rev. Lett.* **77**, 4980 (1996); A. Turlapov, A. Tonyushkin, and T. Sleator, *Phys. Rev. A* **68**, 023408 (2003).
 - [13] M. Weitz, T. Heupel, and T. W. Hänsch, *Phys. Rev. Lett.* **77**, 2356 (1996).
 - [14] H. Hinderthür *et al.*, *Phys. Rev. A* **56**, 2085 (1997).
 - [15] M. Weitz, T. Heupel, and T. W. Hänsch, *Appl. Phys. B* **65**, 713 (1997).
 - [16] B. Anderson *et al.*, *Phys. Rev. A* **63**, 023404 (2001).